Saffman–Taylor instability in yield stress fluids

2005 J. Phys.: Condens. Matter 17 S1219

(http://iopscience.iop.org/0953-8984/17/14/011)

INSTITUTE OF PHYSICS PUBLISHING JOURNAL OF PHYSICS: CONDENSED MATTER

J. Phys.: Condens. Matter **17** (2005) S1219–S1228 doi:10.1088/0953-8984/17/14/011

Saffman–Taylor instability in yield stress fluids

Nahid Maleki-Jirsaraei[1,2], Anke Lindner[3], Shahin Rouhani[4] and Daniel Bonn[1,5]

[1] Laboratoire de Physique Statistique, Ecole Normale Supérieure, 24, Rue Lhomond, F-75231 Paris Cedex 05, France
[2] Complex Systems Laboratory, Physics Department, Azzahra University, Tehran, Iran
[3] LMDH-PMMH, Ecole de Physique et Chimie de la Ville de Paris, 10 rue Vauquelin, 75231 Paris Cedex 05, France
[4] Physics Department, Sharif University of Technology, Tehran, Iran
[5] van der Waals–Zeeman Instituut, Valckenierstraat 65, 1018 XE Amsterdam, The Netherlands

Received 31 July 2004, in final form 21 September 2004
Published 24 March 2005
Online at stacks.iop.org/JPhysCM/17/S1219

Abstract

Pushing a fluid with a less viscous one gives rise to the well known Saffman–Taylor instability. This instability is important in a wide variety of applications involving strongly non-Newtonian fluids that often exhibit a yield stress. Here we investigate the Saffmann–Taylor instability in this type of fluid, in longitudinal flows in Hele–Shaw cells. In particular, we study Darcy's law for yield stress fluids. The dispersion equation for the flow is similar to the equations obtained for ordinary viscous fluids but the viscous terms in the dimensionless numbers conditioning the instability now contain the yield stress. This also has repercussions on the wavelength of the instability as it follows from a linear stability analysis. As a consequence of the presence of yield stress, the wavelength of maximum growth is finite even at vanishing velocities. We study Darcy's law and the fingering patterns experimentally for a yield stress fluid in a linear Hele–Shaw cell. The results are in rather good agreement with the theoretical predictions. In addition we observe different regimes that lead to different morphologies of the fingering patterns, in both rectangular and circular Hele–Shaw cells.

1. Introduction

The so-called Saffman–Taylor instability has received much attention as an archetype of pattern forming systems, both theoretically and experimentally [1–3]. Most natural and industrial materials are non-Newtonian fluids. It is thus also important from a practical point of view to understand the instability in such 'complex fluids'. Lately, this instability has also been studied for non-Newtonian fluids, for which strikingly different fingering patterns are found. The physical origin of the very different structures is so far ill understood, mainly because

most of these fluids exhibit multiple visco-elastic characteristics, which were not determined simultaneously. Very recently, fingering in yield stress fluids was studied both theoretically [4] and experimentally [5]. The theory on yield stress fluids has revealed that the Saffman–Taylor instability is modified drastically. Notably, as a consequence of the presence of yield stress, the wavelength of maximum growth is finite even at vanishing velocities, a result that was nicely confirmed by our experiment. Here we investigate the instability for a typical yield stress fluid: a polymer gel in a linear Hele–Shaw cell. Furthermore, we measure the applied pressure gradient during the viscous fingering experiment. For Newtonian fluids, Darcy's law gives the proportionality between the applied pressure gradient and the finger velocity. Darcy's law is the starting point of all theoretical treatments of the Saffman–Taylor instability. It is thus also important to study its applicability to non-Newtonian fluids, which we do in the present experiment.

2. Experiments and results

2.1. Characterization of the gel

As a yield stress fluid, we use a water based polymer gel[6] at different dilutions. To obtain the visco-elastic properties of the gel, a rheological study is done. Figure 1(a) depicts the shear stress as a function of the shear rate obtained using a Coutte geometry on a Reologica Stress Tech Reometer for a series of dilutions of the gel. It turns out that the flow behaviour of the gel is very well described by the Herschel–Bulkley model:

$$\sigma = \sigma_y + k_1 \dot{\gamma}^n \tag{1}$$

in which σ is the shear stress and $\dot{\gamma}$ is the shear rate. The shear thinning exponent, n, is found to be close to 0.4 for all dilutions (figure 1).

2.2. Experimental set-up

The experiments were performed in a rectangular Hele–Shaw cell (figure 3) consisting of two glass plates separated by a thin Mylar space, fixing the plate spacing b at 0.25 or 0.75 mm. The channel width W is chosen to be 4 cm. The cell is filled with gel, and compressed air is used as the, less viscous, driving fluid. The applied pressure can be modified to obtain different finger velocities. The fingers are captured by a CCD camera coupled to a VCR. We also used a circular cell with $b = 0.25$ mm, in which the air is pushed into the gel, from the centre (figure 7).

2.3. Darcy's law

For Newtonian fluids, the relation between the velocity of the finger and the applied pressure gradient is derived in a trivial way from the Navier–Stokes equation. For the specific geometry of the Hele–Shaw cell, neglecting the inertial term for slow flow between the two glass plates under an applied pressure gradient, one can average the parabolic velocity profile over the gap to obtain

$$v = -b^2/(12\mu)\nabla p \tag{2}$$

μ is the viscosity of the viscous fluid, b the plate spacing and v the average velocity of the fluid far away from the finger. To treat the Saffman–Taylor instability for non-Newtonian fluids, one

[6] Commercial hair gel: 'HEMA' XX strong.

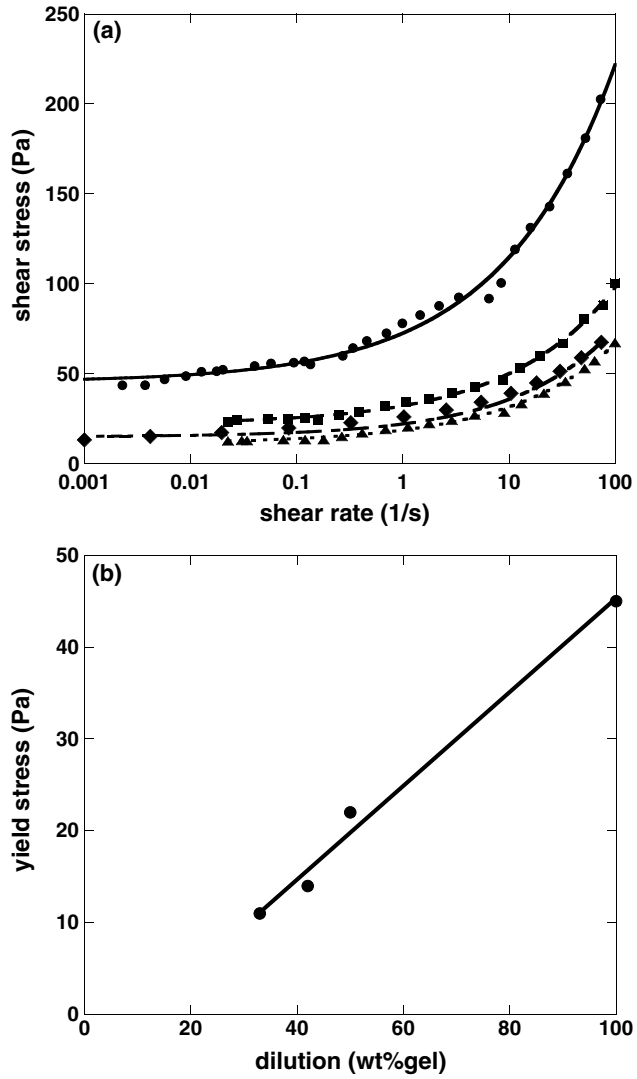

Figure 1. (a) Shear stress as a function of shear rate for different dilutions of the gel. 100 wt% (dots) gel, 50 wt% gel (squares), 42 wt% gel (diamonds) and 33 wt% gel (triangles). (b) Yield stress as a function of the gel and linear fit to the data.

may attempt to replace the constant viscosity μ by a shear dependent viscosity $\mu(\dot{\gamma})$ leading to a modified Darcy law:

$$v = -b^2/(12\mu(\dot{\gamma}))\nabla p. \tag{3}$$

This modified Darcy law is widely used [6, 7]. Kondic *et al* [8, 9] have shown theoretically that, for weak shear thinning (and in the absence of a yield stress), one may replace the constant Newtonian viscosity by a shear-thinning viscosity in order to obtain this modified flow equation, which is verified experimentally for weak shear thinning [10]. Our viscous fingering experiment allows us to perform a direct experimental study of the validity of the modified Darcy law for yield stress fluids.

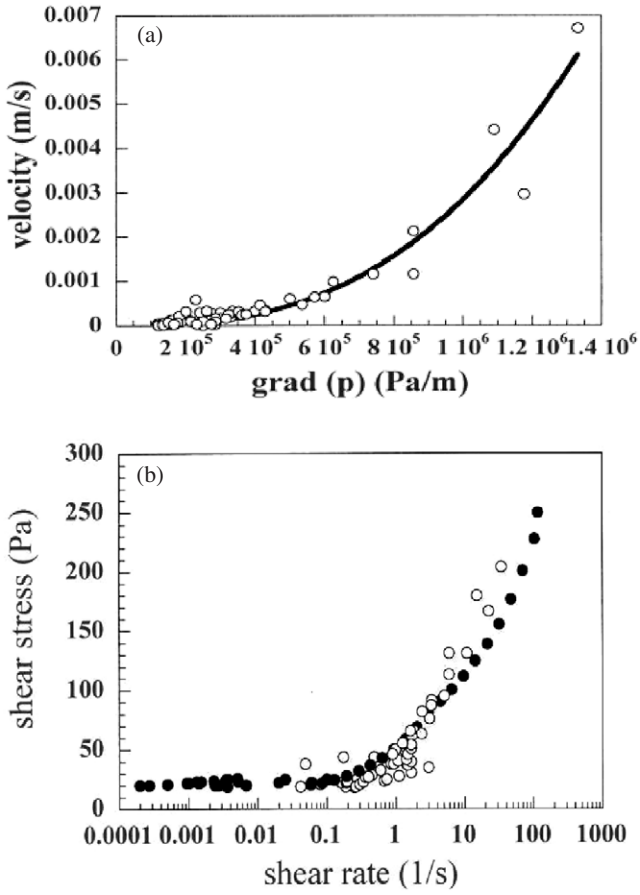

Figure 2. Darcy's law: (a) average velocity versus applied pressure gradient and power law fit to the data. (b) Shear stress as a function of the shear rate from viscous fingering experiments (empty circles) and rheological measurements (filled circles).

We thus study the relation between v and the applied pressure gradient. The pressure gradient is defined as $\nabla p = \Delta p/\Delta l$. The outlet of the cell is at the atmospheric pressure p_0 and the entrance is at the applied pressure p (measured with a standard manometer). The pressure in the finger can be considered to be constant and equals the applied pressure p. Δl is the distance between the finger tip and the outlet of the cell. The plotting of v as a function of ∇p is shown in figure 2(a). Qualitatively, it can be observed that for the gel v is *not* a linear function of ∇p, in contrast to the case for a Newtonian fluid. Quantitatively, the relation between v and ∇p can be compared to the predictions of the modified Darcy law (equation (3)). To do so, we calculate μ from equation (2) for every point $v(\nabla p)$ measured. The average shear rate in the Hele–Shaw cell for a certain v is obtained by taking the average of the velocity gradient of the parabolic flow profile over the spacing between the two plates; in this way, one obtains $\dot{\gamma} = 3v/b$. This leads to results of the form $\mu(\dot{\gamma})$, or identically $\sigma(\dot{\gamma})$ which can be compared directly to rheological measurements of the shear-rate-dependent viscosity. This is done in figure 2(b), from which it is clear that the results of the two independent experiments are in good agreement with each other. The modified Darcy law (equation (3)) thus seems to be well satisfied.

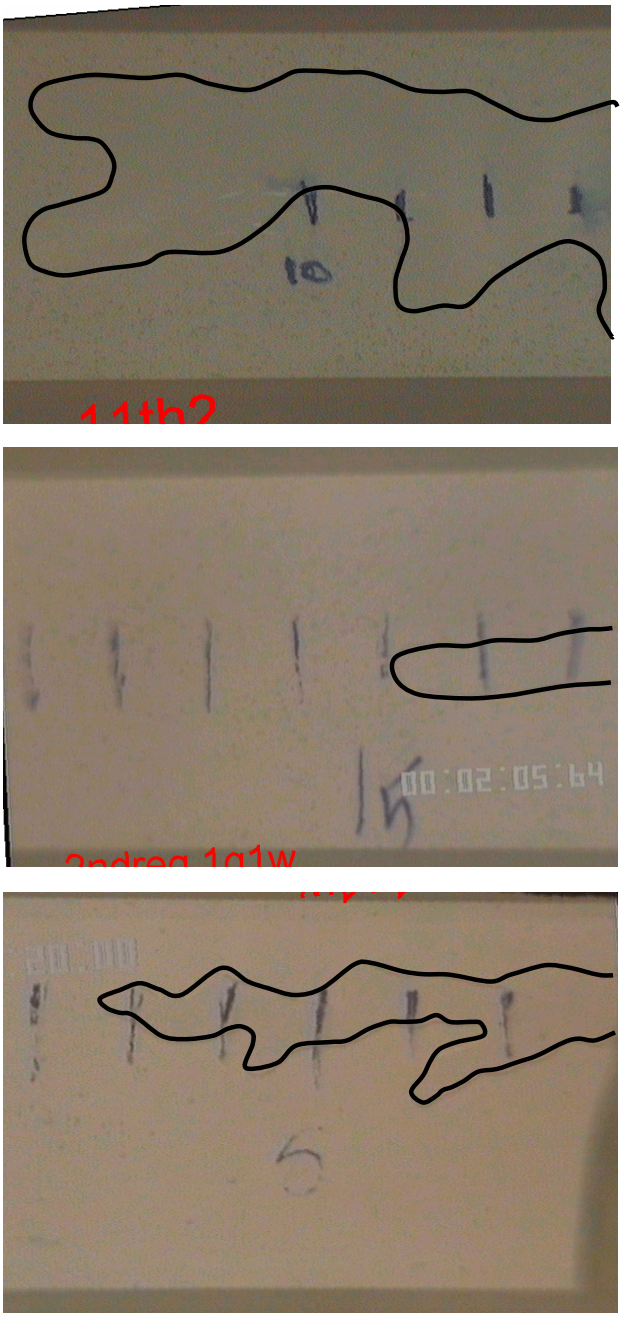

Figure 3. Snapshots of the observed fingering patterns in a 50 wt% dilution: yield stress regime (top) and viscous regime (middle) and side-branching regime (bottom).

2.4. Viscous fingering in a linear Hele–Shaw cell

The viscous fingering experiments are performed in a rectangular Hele–Shaw cell consisting of two glass plates separated by a thin Mylar spacer, fixing the plate spacing b at 0.25 mm. The channel width W is chosen to be 4 cm. The cell is filled with gel, and compressed air is used

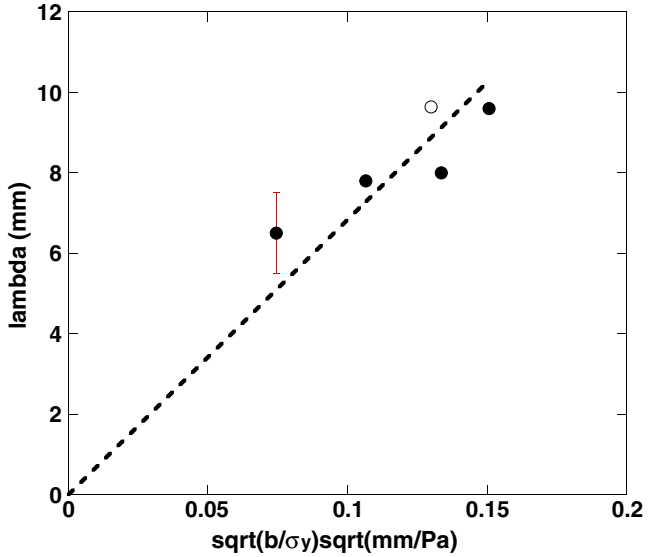

Figure 4. Wavelength measured in the yield stress regime when changing the yield stress. Dilation (closed circles) of 100 wt%, 50 wt%, 42 wt% and 33 wt% of gel are shown keeping the plate spacing $b = 0.25$ mm unchanged. Wavelength (open circle) for a plate spacing of $b = 0.75$ mm and 100 wt% of gel.

as the, less viscous, driving fluid. The applied pressure can be modified to obtain different finger velocities. The fingers are captured by a CCD camera coupled to a VCR. This allows for measurements of the width w as a function of the velocity v of the finger.

For very low velocities ($v < 0.01$ cm s^{-1}) we find ramified structures of the fingers; for low velocities only one finger continues to propagate through the cell, in the middle of the channel. Figure 3 shows the three regimes for the 50% diluted gel. For low velocities ($v < 0.03$ cm s^{-1}) the finger width does not depend on the finger velocity. For higher velocities ($v > 0.1$ cm s^{-1}) the finger width decreases with the finger velocity. A third regime appears when we lower the yield stress. At higher speeds ($v > 2$ cm s^{-1}), the single finger propagating in the middle of the cell destabilizes to form a ramified pattern, as shown in figure 3.

2.4.1. Yield stress regime. For a Newtonian fluid, the most unstable wavelength that follows from the linear stability analysis is

$$\lambda \approx b\sqrt{\left(\frac{\gamma}{U\mu}\right)} \tag{4}$$

in which γ is the surface tension. The total viscous stress can be approximated as $\sigma \approx \mu U/b$ where the shear rate is approximated by $\dot{\gamma} \approx U/b$. For a yield stress fluid, the total stress is given by equation (1), which in the limit of $U \to 0$ yields $\sigma = \sigma_y$. If we now simply replace the viscous stress in equation (4) by the yield stress, we obtain

$$\lambda \approx \sqrt{\frac{b\gamma}{\sigma_y}}. \tag{5}$$

So if we identify λ with the finger width, it should vary as the square root of the plate spacing, and the inverse square root of the yield stress. Figure 4 presents the results for the finger

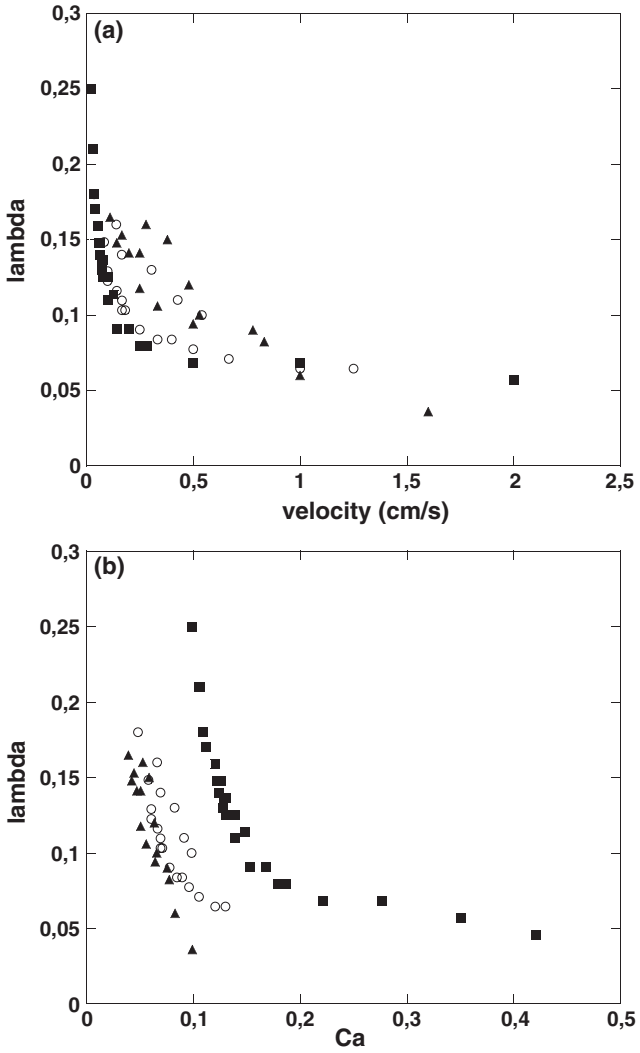

Figure 5. (a) Lambda as a function of the finger velocity U measured in the viscous regime for different dilutions of the gel: 100 wt% (squares), 50 wt% (circles) and 33 wt% (triangles), (b) Lambda as a function of the capillary number Ca in the viscous regime for different dilutions of the gel: 100 wt% (squares), 50 wt% (circles) and 33 wt% (triangles).

width as a function of the new control parameter suggested by equation (5). The agreement is favourable.

2.4.2. Viscous regime. For higher velocities (see figure 1(a)); the fluid behaves like an ordinary viscous fluid which exhibits shear thinning. The power index n of the Herschel–Bulkley model (equation (1)) is found to be $\approx$0.4 for all dilutions. The data for the finger width are summarized in figure 5, from which it is evident that the finger width in the viscous regime decreases with increasing finger velocity and that the relative finger width $\lambda = w/W$ is much smaller than the classical limit $\lambda = 0.5$. When trying to rescale the results on $1/B = Ca\,(W/b)^2$ ($Ca = \mu U/\gamma$ is the capillary number), the control parameter for Newtonian fluids, where the viscosity has been replaced by the shear thinning viscosity, one finds that

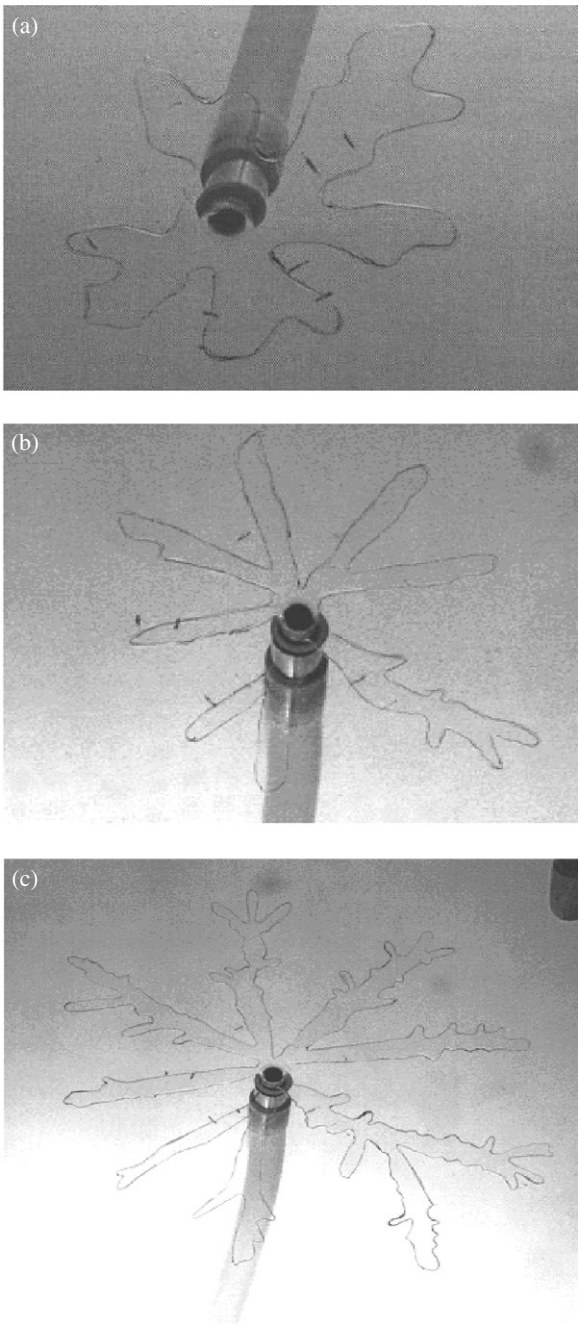

Figure 6. Snapshots of the fingering patterns observed in the circular cell for the undiluted gel: (a) yield stress regime, (b) viscous regime and (c) side-branching regime.

the results do not collapse onto a single curve. This is surprising, since although the yield stress can be very different for the different dilutions of the gel, the shear-thinning exponent is not (figure 1(a)). We must therefore conclude that the observed difference between the different dilutions is due to another effect. The effect of normal stresses, if present, leads to

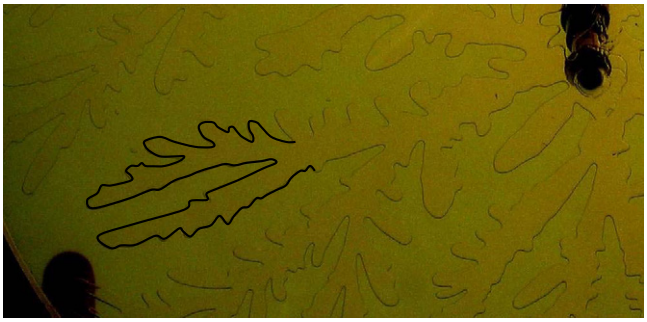

Figure 7. Snapshot of a 'dublon' in the undiluted gel in the circular cell.

larger fingers [11, 12]. Rheology measurements indeed reveal the presence of normal stresses, which of course become less important if the gel is more diluted; this seems to be a plausible explanation for the differences observed in figure 5.

2.4.3. Side-branching regime. In this regime, the speeds are high; therefore, it seems likely that yield stress effects are completely absent; we are effectively dealing with a shear-thinning fluid. If the control parameter $1/B = Ca\ (W/b)^2$ becomes larger than a certain value ($1/B \approx 5000$, in general) the finger becomes unstable against tip splitting [13]. For the gel, we occasionally do observe tip splitting, but the observed ramifications mainly come from side-branching instabilities (figure 3). This is in fact a typical observation made for shear-thinning fluids [12]: shear thinning stabilizes the finger tip against tip splitting. Suppression of tip splitting is also found theoretically for shear-thinning fluids [14, 15].

2.5. Viscous fingering in circular geometry

The three regimes presented in the rectangular cell have also been recognized in our experiment in the circular Hele–Shaw cell. The results are summarized in figure 6. We have also observed the so-called dublon effect at very high velocities which was observed formerly in the solidification (figure 7).

3. Discussion and conclusion

We have demonstrated that the Saffman–Taylor instability is drastically modified in yield stress fluids. We identify three different regimes that lead to different morphologies of the fingering patterns. The presence of a yield stress leads to very branched patterns at low velocity, where the yield stress plays an important role. For somewhat higher velocities only a single stable finger is observed. At even higher speeds, the finger propagation in the centreline of the cell destabilizes and undergoes side-branching instabilities.

The results in the yield stress regime can be understood quantitatively from a linear stability analysis. The repercussion on the wavelength of the instability as it follows from a linear stability analysis is that the wavelength of maximum growth is finite even at vanishing velocities. The results in the second and third regimes are more difficult to understand in a quantitative fashion. Here, we find different behaviours for the different dilutions of the gel, having nonetheless very similar shear-thinning exponents. We propose that the differences might be due to normal stress effects [11]. For the third regime, the side-branching instabilities

are non-linear secondary instabilities that are not fully understood to date; therefore, a quantitative comparison with theory is impossible.

We propose a modified Darcy law (equation (3)). The effective viscosity can be compared directly to the rheological measurements of the shear-rate-dependent viscosity; the main result is that the results of the two independent experiments agree well with each other, and use of the modified Darcy law (equation (3)) is therefore justified.

We have also recognized the mentioned three regimes in a circular Hele–Shaw cell. We have also observed the dublon effect at very high velocities, an effect which was observed before in the solidification and other problems of directional growth (figure 7). In sum, although our systematic study of fingering in a well characterized system that exhibits a yield stress helps us to understand some of the previous observations on fingering in complex fluids, a few puzzling observations remain without explanation.

Acknowledgments

NM and DB are very grateful to Professor Keith Moffat, who made it possible for NM to visit the LPS. LPS de l'ENS is UMR 8550 of the CNRS, associated with the universities Paris 6 and Paris 7.

References

[1] Saffman P G and Taylor G I 1958 *Proc. R. Soc.* A **245** 312
[2] McLean J W and Saffman P G 1981 *J. Fluid Mech.* **102** 455
[3] Combescot R C, Dombre T, Hakim V and Pomeau Y 1986 *Phys. Rev. Lett.* **56** 2036
[4] Coussot P 1999 *J. Fluid Mech.* **380** 363
[5] Lindner A, Coussot P and Bonn D 2000 *Phys. Rev. Lett.* **85** 314
[6] Ben Amar M 1995 *Phys. Rev.* E **51** 3819
[7] Sader J E, Chan D Y C and Hughes B D 1994 *Phys. Rev.* E **49** 420
[8] Kondic L, Shelley M J and Palffy-Muhoray P 1998 *Phys. Rev. Lett.* **80** 1433
[9] Kondic L, Palffy-Muhoray P and Shelley M J 1996 *Phys. Rev.* E **54** R4536
[10] Lindner A, Bonn D and Meunier J 2000 *Phys. Fluids* **12** 256
[11] Bonn D and Meunier J 1997 *Phys. Rev. Lett.* **79** 2662
[12] Lindner A 2002 *J. Fluid Mech.* **469** 237
[13] Bensimon D, Kadanoff L P, Liang S, Shraiman B I and Tang C 1986 *Rev. Mod. Phys.* **58** 977
[14] Fast P *et al* 2001 *Phys. Fluids* **13** 1191
[15] Fast P and Shelly M J 2004 *J. Comput. Phys.* **195** 117